IBRO Neuroscience Reports 18 (2025) 592–603

Contents lists available at ScienceDirect

IBRO Neuroscience Reports

journal homepage: www.sciencedirect.com/journal/IBRO-Neuroscience-Reports

Distribution of mRNA for the exocytotic calcium sensor, synaptotagmin 9, in mouse brain

Kwadwo O. Boateng [a,b,1], Lucian D. Hadford [c,1], Kelly L. Stauch [d], Anthony E. Kincaid [e], Wallace B. Thoreson [a,f,*]

[a] Integrative Physiology and Molecular Medicine Graduate Program and University of Nebraska Medical Center, Omaha, NE, USA
[b] Department of Ophthalmology and Visual Sciences, University of Nebraska Medical Center, Omaha, NE, USA
[c] University of Nebraska – Omaha, Omaha, NE, USA
[d] Department of Neurological Sciences, University of Nebraska Medical Center, Omaha, NE, USA
[e] Department of Pharmacy Sciences, Creighton University, Omaha, NE, USA
[f] Department of Pharmacology and Experimental Neuroscience, University of Nebraska Medical Center, Omaha, NE, USA

ARTICLE INFO

Keywords:
Synaptotagmin 9
RNAscope
Mouse brain

ABSTRACT

The principal Ca^{2+} sensors that control fusion of synaptic vesicles are synaptotagmins 1, 2 and 9. Synaptotagmin 9 (Syt9) has received the least attention. We applied RNAscope techniques to coronal sections of adult mouse brain to study the distribution of Syt9 mRNA. Our results showed weak Syt9 mRNA expression in many brain regions but elevated levels in a handful. Regions of strong expression were largely in limbic and sensory areas and included both excitatory and inhibitory neurons. Strongest expression in the brain was in the medial habenula. The interpeduncular nucleus that provides input to medial habenula and amygdala that receives medial habenula output also showed elevated Syt9 mRNA. Sensory regions with strong Syt9 mRNA expression included mitral and periglomerular cells in the olfactory bulb, thalamus, and sensory layers of the superior colliculus. A few putative layer 5 pyramidal cells in somatosensory, auditory and visual cortex were also strongly labeled. Neurons in motor regions including cortex did not generally show elevated expression with the exception of strong labeling of granular and molecular (but not Purkinje) cells in the cerebellum. Hippocampal neurons also showed only weak labeling.

1. Introduction

Calcium-dependent fusion of synaptic vesicles and release of neurotransmitters at neuronal synapses is regulated by specific Ca^{2+} sensor molecules. Synaptotagmin (Syt) serves as the primary Ca2 + sensor for exocytosis at most synapses (Mackler et al., 2002; Fernandez-Chacon et al., 2001; Brose et al., 1992; Geppert et al., 1994; Xu et al., 2007). While 17 Syt homologs have been identified in mouse and human, only 8 bind Ca^{2+}: Syt1–3, 5–7, 9, and 10 (Bhalla et al., 2006; Bhalla et al., 2005; Pinheiro et al., 2016; Craxton, 2010; Sugita et al., 2002; Li et al., 1995; Hui et al., 2005). Among these, Syt 1, 2 and 9 show the lowest Ca^{2+} affinity (EC50 ~10–20 μM) and are thought to be the Ca^{2+} sensors that control fast, synchronous release in most CNS neurons (Geppert et al., 1994; Pang et al., 2006; Xu et al., 2007). Of these three, Syt2 shows the fast kinetics and Syt9 the slowest (Wolfes and Dean, 2020). Consistent with their important roles in neurotransmission, mutations in these proteins can cause neurological impairments (Verhage and Sorensen, 2020; Monies et al., 2017).

Of the three key Ca^{2+} sensors, Syt9 is the least studied. Syt9 levels assessed by qPCR in the brain are substantially lower than Syt1 overall, but elevated in a few distinct regions. In situ hybridization experiments showed high levels of Syt9 mRNA in thalamus, cerebellum, olfactory bulb, and medial habenula (Mittelsteadt et al., 2009) (Allen Brain Atlas; https://mouse.brain-map.org/gene/show/37970). Expression of GFP-tagged Syt9 protein in a knock-in mouse model showed strong expression in striatum, olfactory bulb, and hypothalamus (Xu et al., 2007) and Syt9 can regulate both evoked and spontaneous release from striatal neurons (Seibert et al., 2023; Xu et al., 2007). Syt9 mRNA is also elevated in bipolar cells of the retina (Mesnard et al., 2024). In this study, we characterized Syt9 mRNA distribution in coronal sections of

* Correspondence to: Truhlsen Eye Institute, Durham Research Center 1, University of Nebraska Medical Center, Room 4050, Omaha, NE 68198-5840, USA.
E-mail address: wbthores@unmc.edu (W.B. Thoreson).
[1] Both authors contributed equally.

https://doi.org/10.1016/j.ibneur.2025.03.009
Received 4 February 2025; Received in revised form 25 March 2025; Accepted 27 March 2025
Available online 2 April 2025

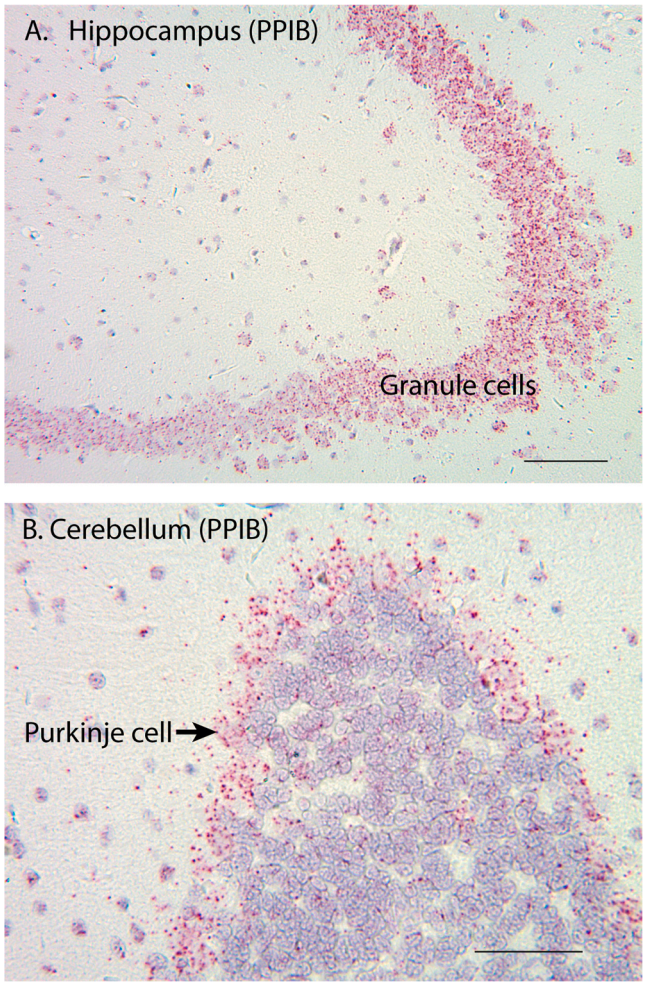

Fig. 1. RNAscope labeling for PPIB (cyclophilin B) was used as a positive control. A) Strong labeling for PPIB was evident in hippocampal granule cells although these cells showed little or no labeling for Syt9 mRNA. B) Strong labeling for PPIB was also present in cerebellar Purkinje cells that showed little or no labeling for Syt9 mRNA. Scale bar = 50 μm.

mouse brain used RNAscope methods for improved cellular resolution.

2. Material and methods

2.1. Mice

We examined mRNA in C57Bl6J mice (Jackson Labs.). We show results from 3 adult mice (6–16 weeks, 2 males, 1 female). We saw no obvious differences in RNAscope labeling for Syt9 between male and female mice, but a much larger sample would be needed to establish this more conclusively. Euthanasia was conducted in accordance with AVMA Guidelines for the Euthanasia of Animals by CO2 asphyxiation followed by cervical dislocation. Animal care and handling protocols were approved by the University of Nebraska Medical Center Institutional Animal Care and Use Committee.

2.2. RNAscope

Brains were fixed in 4 % paraformaldehyde (PFA) for 48 hours, transferred to 70 % ethanol, and processed for paraffin embedding. Five micron thick sections were cut by the UNMC Tissue Sciences Facility. Additional processing steps were performed using the RNAscope™ 2.5 HD Reagent Kit (RED) and the Quick Guide for FFPE Tissues (Advanced Cell Diagnostics, Newark, CA, RRID:SCR_012481; Cat No: 322350).

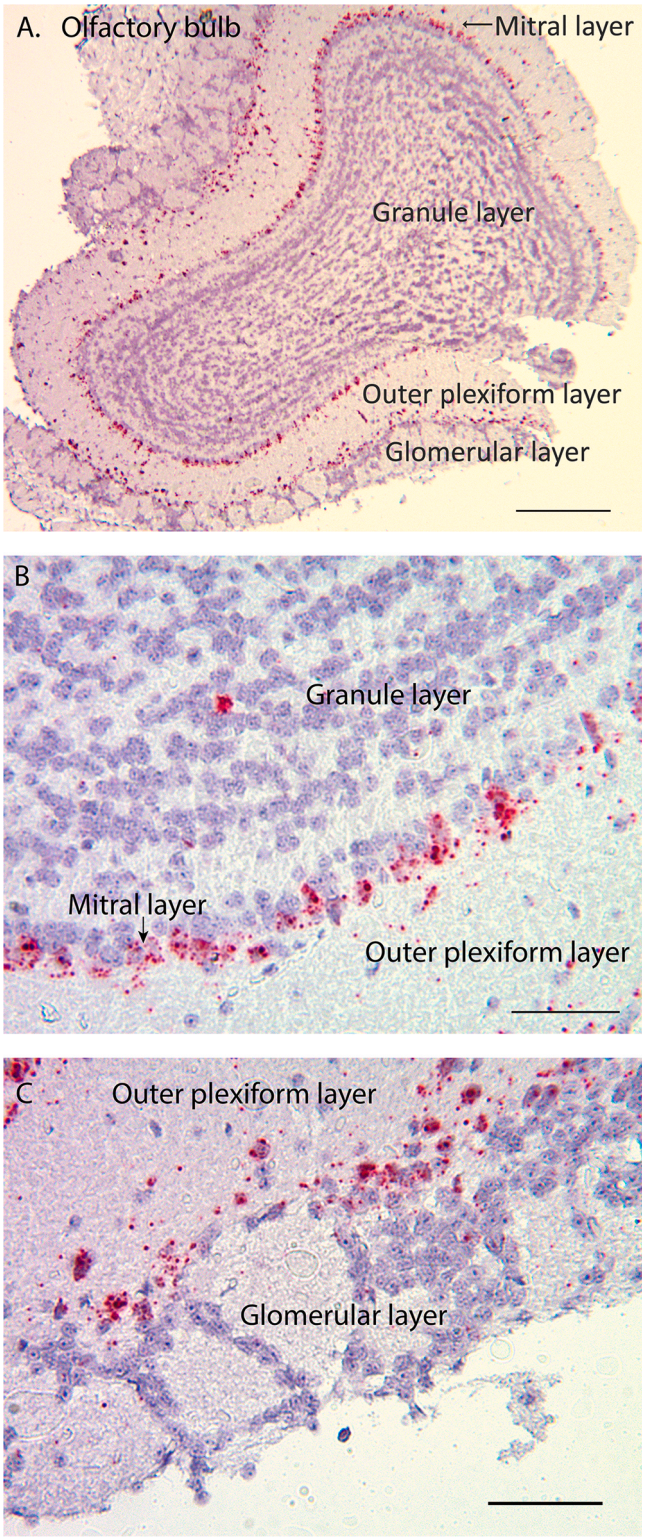

Fig. 2. Olfactory bulb at lower (A, scale bar = 0.5 mm) and higher (B, C, scale bar = 50 μm) magnification. Panel B shows the granule, mitral and outer plexiform layers while panel C focuses on the outer plexiform and glomerular layers. This coronal section was cut at a level equivalent to section 11 in coronal sections from the mouse Allen Brain Atlas (https://mouse.brain-map.org/experiment/thumbnails/100048576?image_type=atlas). Syt9 mRNA labeled by RNAscope methods appears as red puncta.

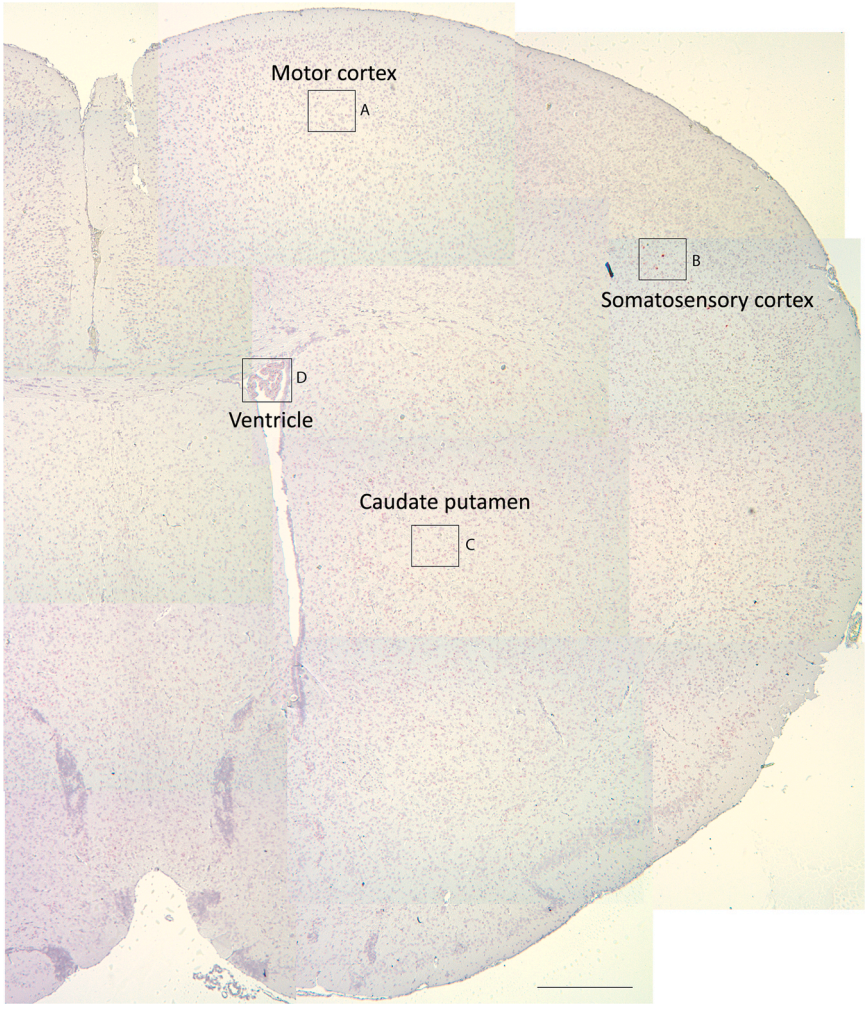

Fig. 3. Composite image of coronal mouse brain at level 45 of the Allen Brain Atlas. Boxes enclose regions of primary motor cortex (A), primary somatosensory cortex (B), caudate putamen (C), and ventricle (D). These regions are shown at higher magnification in Fig. 3. Scale bar = 0.5 mm.

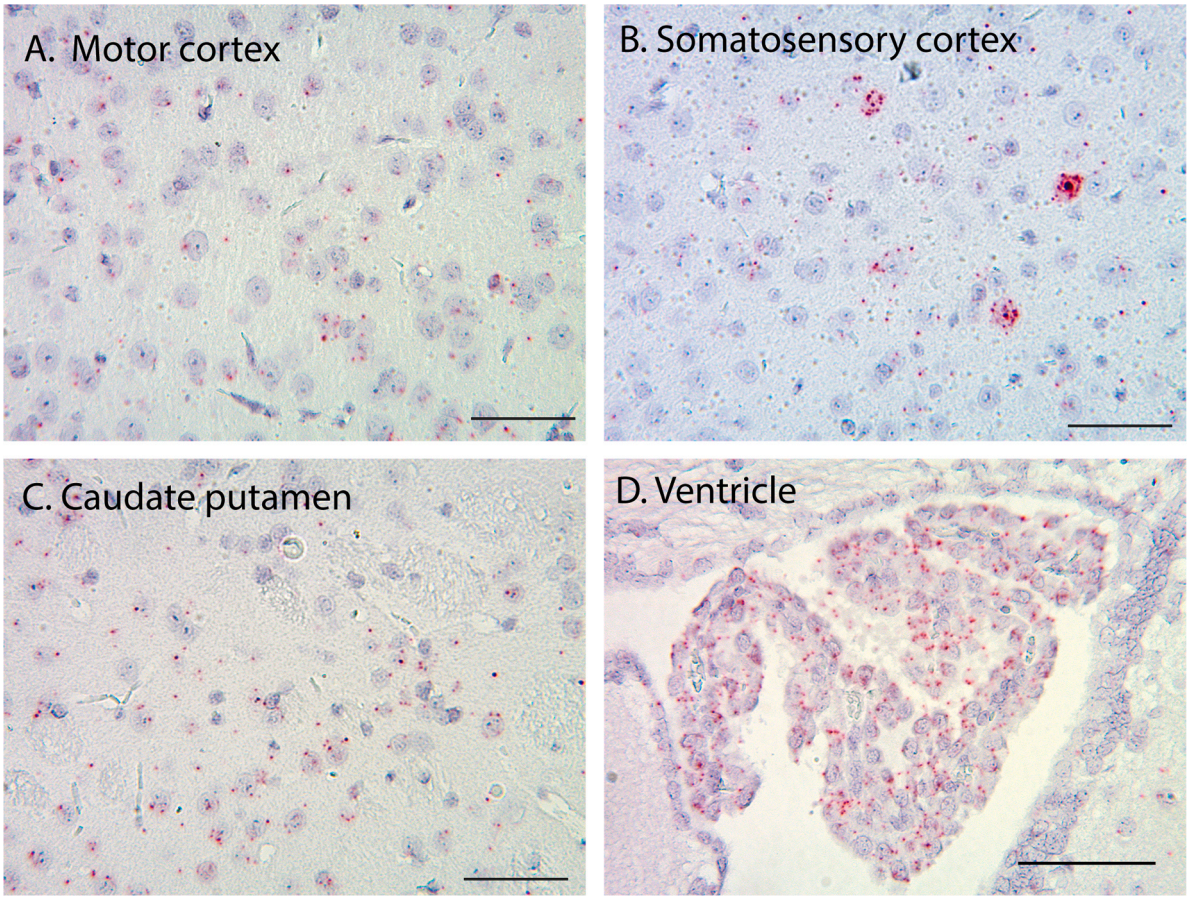

Fig. 4. Higher magnification images of regions enclosed by boxes in Fig. 2. A) primary motor cortex, B) primary somatosensory cortex, C) caudate putamen, and D) ventricle. Scale bar = 50 μm.

Sections were baked at 60° C and then deparaffinized in a series of xylene and 100 % ethanol baths at room temperature. Slides were set to air dry for 5 minutes to prepare for pretreatment. Pretreatment of slides included direct application of hydrogen peroxide to tissue sections for 10 minutes followed by consecutive distilled water washes. Sections were submerged in Target Retrieval solution at 95–100° C and sustained by a hot water bath for heat-induced antigen retrieval. Before in situ hybridization, tissue was digested using Protease Plus enzyme solution at 40°C in a humidity chamber.

In situ hybridization for Syt9 RNA was performed using probes targeting Syt9 (Advanced Cell Diagnostics, Newark, CA). Probe Mm-Syt9 (Cat No. 845291) targets the base pair region 636–1595 of the Syt9 transcript (NCBI accession number NM_021889.4). This target region includes a portion of exon 2; the entirety of exons 3, 4, and 5; and a portion of exon 6. Target amplification and color development were done using the 2.5 HD Red Detection sub-kit, which involved a series of six amplifications and incubations with intermittent washes (ACD Bio Cat No. 310091). Visualization was achieved by applying Fast Red dye and counterstaining sections with Hematoxylin QS (Vector Laboratories, Burlingame, CA). Tissue was then dried at 60° C before a 15-second xylene dip and subsequent mounting in EcoMount medium (Biocare Medical, Cat. No. EM897L).

RNAscope labeling for PPIB (cyclophilin B) was used as a positive control. According to Advanced Cell Diagnostics (RRID:SCR_012481) literature, PPIB is typically expressed at 10–30 copies per cell. Fig. 1A shows an example of strong labeling for PPIB in hippocampal granule cells (although these cells showed little or no labeling for Syt9 mRNA). Fig. 1B shows strong labeling for PPIB in cerebellar Purkinje cells (that also showed little or no labeling for Syt9 mRNA).

Images were captured using SPOT Basic software (SPOT Imaging, Diagnostic Instruments Inc.) on a Spot Idea color camera (Diagnostics Instruments, Model 28.2) and Leitz Diaplan upright microscope under 25X and 40X objectives.

3. Results

We examined a series of coronal brain sections, focusing on levels that had shown strong Syt9 protein or mRNA expression in earlier work (Mittelsteadt et al., 2009; Xu et al., 2007). Although we also looked at additional sections while refining techniques, we focused our studies on sections from three mice for more detailed examination. These mice showed similar expression patterns but the small sample limited our ability to assess mouse-to-mouse variability. For reference, we note the equivalent coronal sections in the Allen Mouse Brain Atlas. For example, Fig. 2 shows a section through olfactory bulb cut at level 11 of the coronal sections in the Allen Mouse Brain Atlas (https://mouse.brain-map.org/experiment/thumbnails/100048576?image_type=atlas). RNAscope labeling of Syt9 mRNA appears as red puncta in these images. Consistent with earlier studies (Mittelsteadt et al., 2009; Xu et al., 2007), we saw strong labeling for Syt9 mRNA in olfactory bulb. Panel A shows a lower magnification image while B and C show higher magnification images. RNAscope labeling was particularly strong in the mitral cell layer (Fig. 2B) and in periglomerular cells residing in the outer plexiform layer adjacent to the glomerular layer (Fig. 2C).

Fig. 3 shows a composite image of coronal mouse brain cut at level 45 of the Allen Brain Atlas. Syt9 mRNA expression was relatively low at this level of the brain. One exception to this was elevated expression in the choroid plexus of the ventricle. Fig. 4 shows higher magnification images of the regions indicated by boxes in the composite image of Fig. 3: A) primary motor cortex, B) primary somatosensory cortex, C)

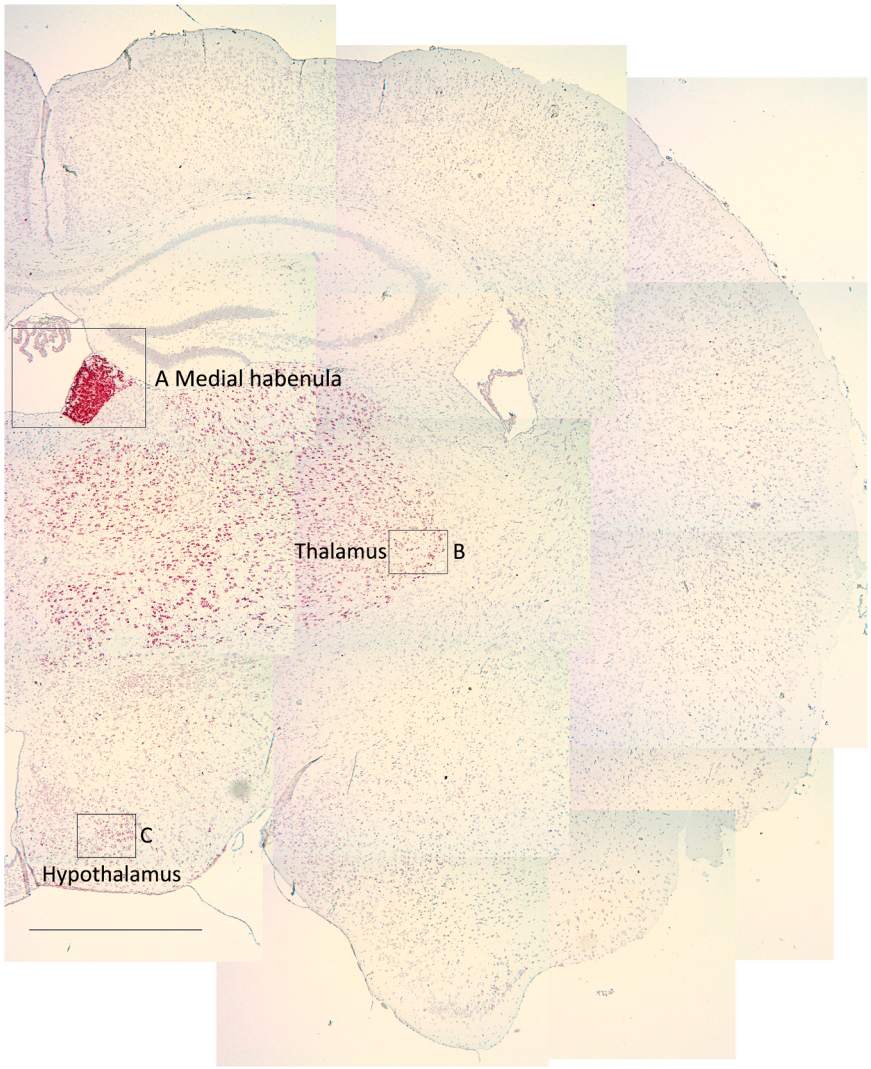

Fig. 5. Composite image of coronal mouse brain at level 71 of the Allen Brain Atlas. Boxes enclose medial habenula (A), regions of ventral posterolateral nucleus and reticular nucleus of the thalamus (B), and ventromedial hypothalamus (C). These regions are shown at higher magnification in Fig. 5. Scale bar = 1 mm.

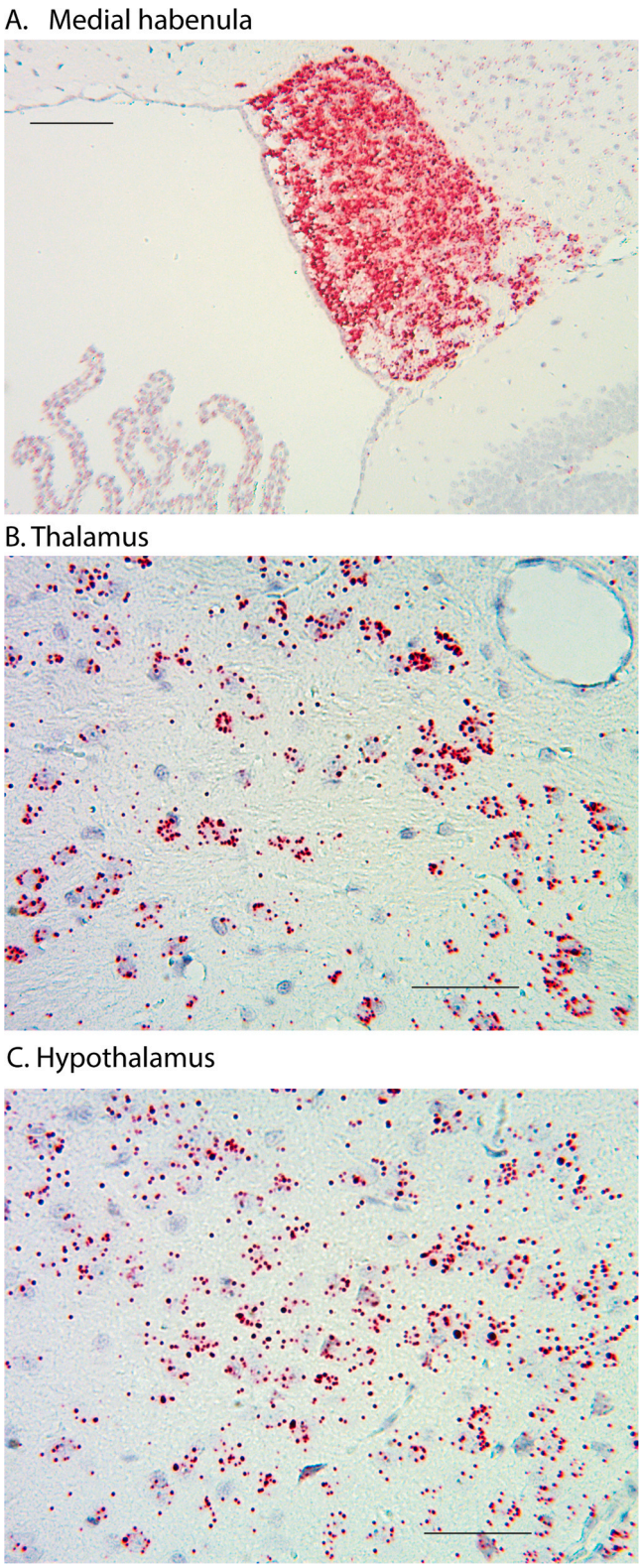

Fig. 6. Higher magnification images of regions enclosed by boxes in Fig. 4. A) medial habenula (scale bar = 100 μm), B) ventral thalamus (scale bar = 50 μm), and C) ventromedial hypothalamus (scale bar = 50 μm).

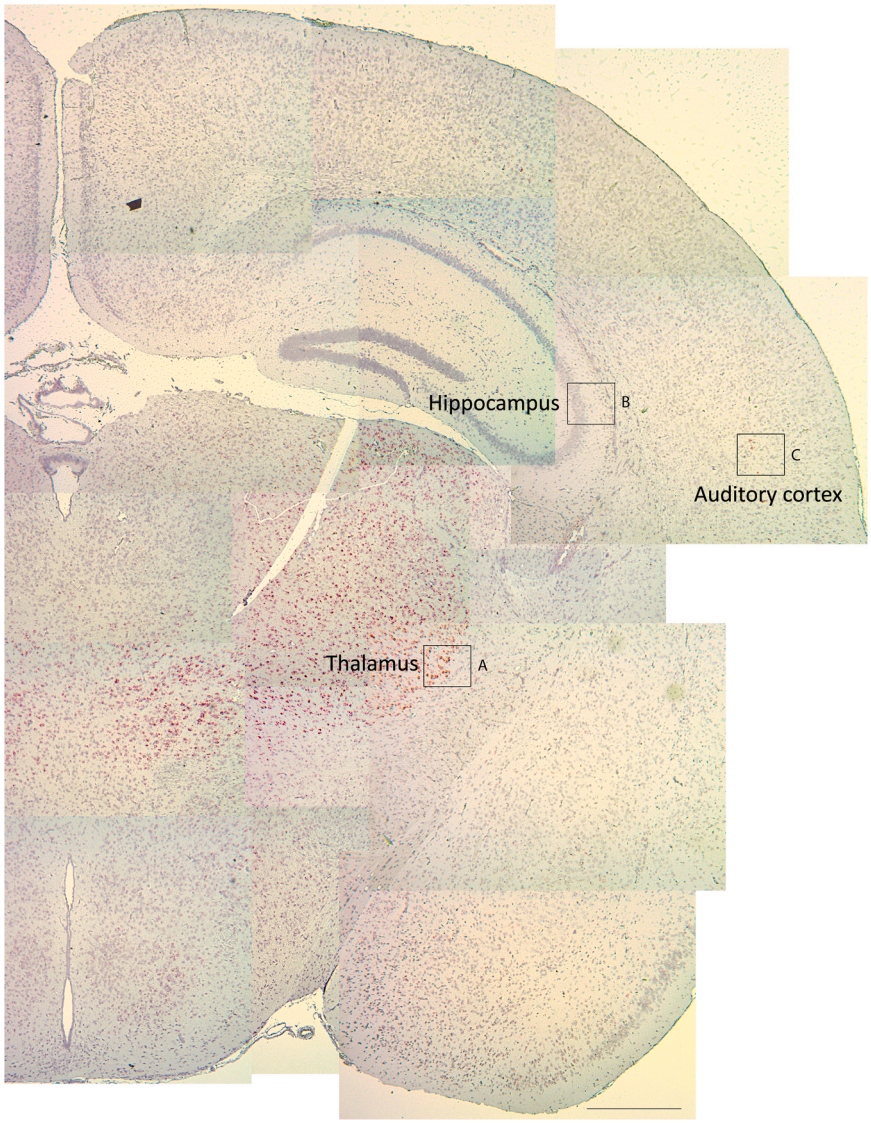

Fig. 7. Composite image of coronal mouse brain at level 78 of the Allen Brain Atlas. Boxes enclose regions of ventral lateral geniculate nucleus of the thalamus (A), CA3 region of hippocampus (B), and layer 5 of auditory cortex (C). These regions are shown at higher magnification in Fig. 7. Scale bar = 0.5 mm.

caudate putamen, and D) ventricle. Most neurons in cortex showed weak labeling but a few large, putative pyramidal neurons in layer 5 of sensory cortex showed strong labeling. Fig. 4B shows an example from somatosensory cortex. Later figures show other examples of strongly labeled layer 5 neurons in auditory and visual cortex. When measured along their long axis, strongly labeled layer 5 cells from these three sensory brain regions averaged 19.1 $\pm$ 4.08 μm (n = 34) in length. Similar strongly labeled cells were not seen in motor cortex (Fig. 4A).

While the caudate putamen showed strong labeling for Syt9 protein (Xu et al., 2007), it showed weak labeling for Syt9 mRNA suggesting that the protein is probably expressed in presynaptic terminals of neurons whose somas reside elsewhere (e.g., thalamus).

Cells in the choroid plexus of the ventricles were strongly labeled, but ependymal cells that line the ventricles were not. The choroid plexus includes both capillary endothelial cells and neuroepithelial cells. Given that the latter arise from a neuroectodermal lineage like neurons, it seems more likely that RNAscope labeling in this figure reflects the presence of Syt9 mRNA in neuroepithelial cells rather than capillary endothelium.

The composite coronal section in Fig. 5 (level 71) shows strong labeling for Syt9 mRNA in thalamus (ventral posterolateral nucleus and reticular nucleus), ventromedial hypothalamus and especially strong labeling in medial habenula. Higher magnification images of the regions enclosed by boxes are shown in Fig. 6. The strongest labeling in the entire brain was seen in medial habenula. As shown in Fig. 4, one can also see Syt9 labeling in the adjacent choroid plexus. Strongly labeled neurons were present throughout almost the entire thalamus, with weaker labeling only seen in the central medial nucleus. Consistent with elevated Syt9 protein expression in this region (Xu et al., 2007), neurons in the ventromedial hypothalamus were also strongly labeled. Labeling is less prominent in lateral hypothalamus.

The coronal section in Fig. 7 (level 78) and corresponding magnified views in Fig. 8 shows additional evidence of strong Syt9 mRNA labeling throughout the thalamus, including both dorsal and ventral lateral geniculate nuclei. Hippocampal labeling was weak. Fig. 8B shows a higher magnification image of the hippocampal CA3 region. A high magnification image of CA1 is shown later. Like somatosensory cortex, most neurons in auditory cortex showed low expression, but a few putative layer 5 pyramidal neurons in primary auditory cortex showed high levels of Syt9 mRNA (Fig. 8C).

Moving further back, Fig. 9 (level 85) shows continued strong labeling in thalamus (medial geniculate) as well as labeling in the interpeduncular nucleus, amygdala, and superficial sensory layers of superior colliculus. Higher magnification images of these regions are shown in

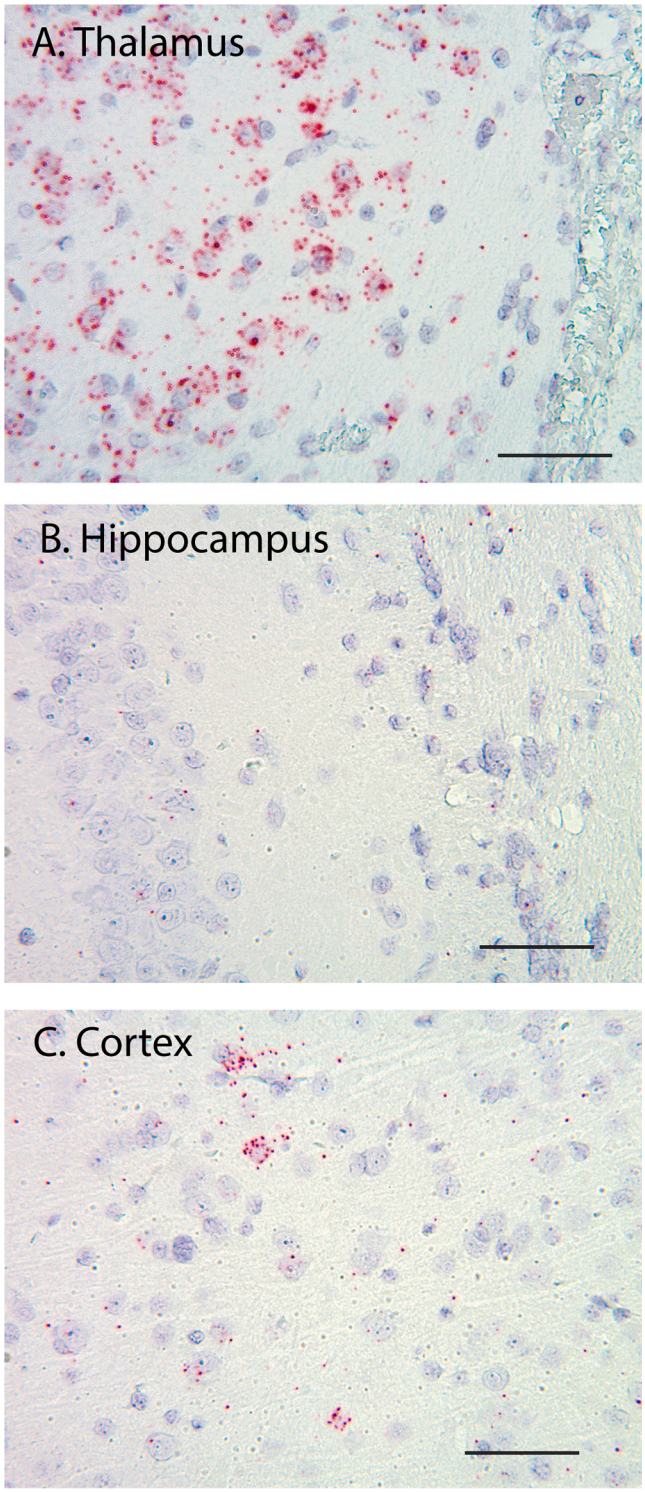

Fig. 8. Higher magnification images of regions enclosed by boxes in Fig. 6. A) ventral lateral geniculate nucleus of the thalamus, B) CA3 region of hippocampus, and C) layer 5 of primary auditory cortex. Scale bar = 50 μm.

Fig. 10. Along with other sensory areas in thalamus, auditory cortex and somatosensory cortex, we saw strong labeling for Syt9 mRNA in sensory, but not motor layers, of superior colliculus (Fig. 10A). And we again saw strong labeling in thalamus (medial geniculate). Like other sensory cortical areas, we saw occasional strong labeling of putative pyramidal neurons in layer 5 of visual cortex (Fig. 10F).

Amygdala provides inputs to medial habenula while the interpeduncular nucleus is a major downstream target of medial habenula neurons. Neurons in the interpeduncular nucleus and amgydala were also both strongly labeled (Fig. 10D). Circuits in these limbic regions are important for regulating motivation and reward (Mclaughlin et al., (2017); Mathis and Kenny, 2019). Like CA3 (Fig. 8B), we saw only weak Syt9 mRNA labeling in CA1 region of hippocampus (Fig. 10E).

Fig. 11 shows a section from posterior brain that included part of the cerebellum (level 106). As shown in the higher magnification image of Fig. 11B, glutamatergic neurons throughout the granular layer and

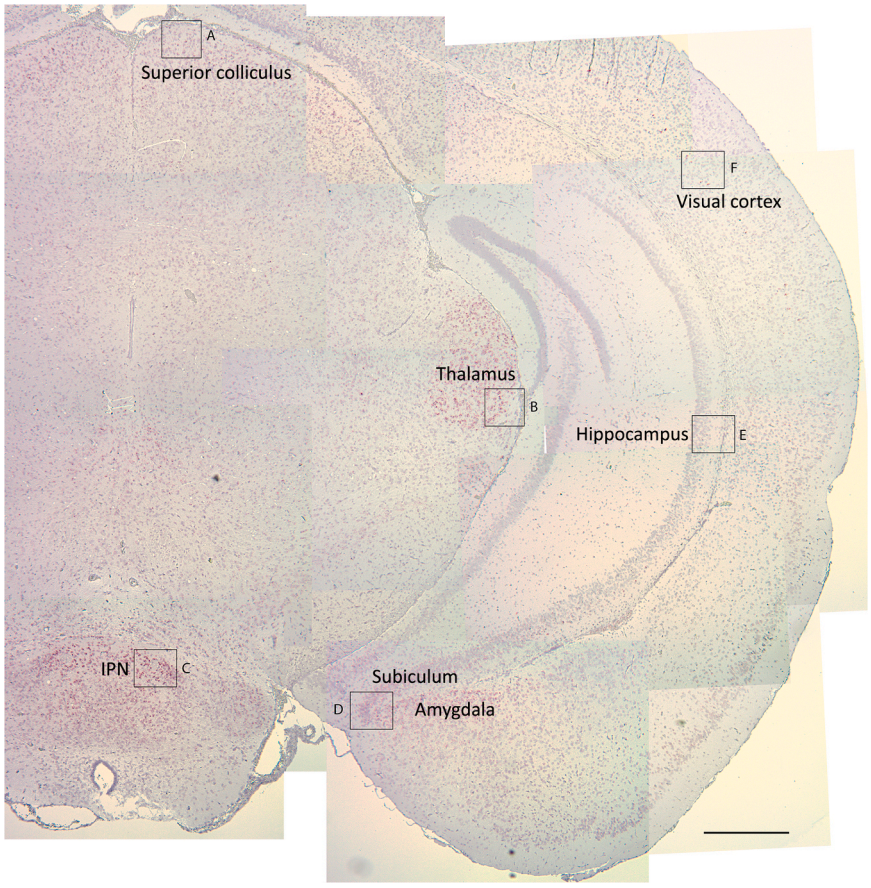

Fig. 9. Composite image of coronal mouse brain at level 85 of the Allen Brain Atlas. Boxes enclose sensory regions of superior colliculus (A), medial geniculate nucleus of the thalamus (B), interpeduncular nucleus (IPN, C), amygdala and adjacent subiculum (D), CA1 region of hippocampus (E), and layer 5 of anterolateral visual cortex (F). These regions are shown at higher magnification in Fig. 7. Scale bar = 0.5 mm.

putative GABAergic stellate cells in the molecular layer were strongly labeled for Syt9 mRNA. Notably, large Purkinje cells that sit at the border between molecular and granular layers were not labeled for Syt9 mRNA.

4. Discussion

Our results are consistent with earlier in situ hybridization results (Mittelsteadt et al., 2009) (Allen Brain Atlas; https://mouse.brain-map.org/gene/show/37970), showing that Syt9 mRNA is expressed at high levels in a handful of brain regions, with stronger expression in sensory and limbic regions and weaker expression in motor regions. RNAscope techniques provide improved sensitivity and specificity compared to traditional in situ hybridization and demonstrate the presence of Syt9 mRNA in both excitatory and inhibitory neurons. For example, Syt9 mRNA levels were elevated in periglomerular neurons and mitral cells of the olfactory bulb that are both thought to be GABAergic (Nagayama et al., 2014). But strong expression of Syt9 mRNA was also present in putative cortical pyramidal cells and cerebellar granule cells that are both thought to be glutamatergic (Carey, 2024). Medial habenula neurons showed particularly strong expression of Syt9 mRNA and neurons in this brain region release both acetylcholine and glutamate (Lee et al., 2019).

A variety of sensory areas show elevated expression of Syt9 mRNA. This included almost the entire thalamus, with the exception of the central medial nucleus, as well as sensory layers of the superior colliculus. Olfactory bulb also showed elevated Syt9 mRNA expression. A subset of large layer 5 neurons in sensory cortex (auditory, somatosensory, and visual), presumably pyramidal cells, were also strongly labeled for Syt9 mRNA. Dendrites of layer 5 pyramidal neurons project to other cortical areas as well as brainstem and midbrain, including thalamus (Moberg and Takahashi, 2022).

Syt9 mRNA showed weaker expression in motor areas including motor cortex, basal ganglia and motor areas of superior colliculus. Syt9 protein is strongly expressed in caudate putamen and has been shown to regulate synaptic release in striatal neurons (Seibert et al., 2023; Xu et al., 2007). However, mRNA levels were surprisingly low in these regions suggesting that dendrites expressing Syt9 protein originate in other structures (e.g., thalamus). While strongly expressed in granule cells of the cerebellum, Syt9 mRNA is largely absent from Purkinje cells that serve as cerebellar output neurons.

Various limbic regions including amygdala, medial hypothalamus, interpeduncular nucleus, and medial habenula also showed strong Syt9 mRNA expression whereas hippocampal neurons in CA1 and CA3 showed only weak labeling for Syt9 mRNA. The strongest expression of Syt9 mRNA in the brain was in medial habenula, consistent with earlier in situ hybridization results (Mittelsteadt et al., 2009). A recent study using single nucleus RNA-seq also showed strong expression of Syt9 mRNA in medial habenula neurons but not oligodendrocytes, microglia, or astrocytes, or lateral habenula neurons (Childs et al., 2024). While Syt9 shows particularly strong expression in medial habenula, in situ hybridization experiments in the Allen Brain Atlas also show evidence for expression of the other major fast exocytotic Ca^{2+} sensors, Syt1 and Syt2, in this structure. The medial habenula conveys signals to the interpeduncular nucleus and receives input from amygdala, both of which showed elevated labeling for Syt9. These regions are important in motivation and reward (Mclaughlin et al., (2017); Mathis and Kenny, 2019) and the medial habenula has been identified as a particularly

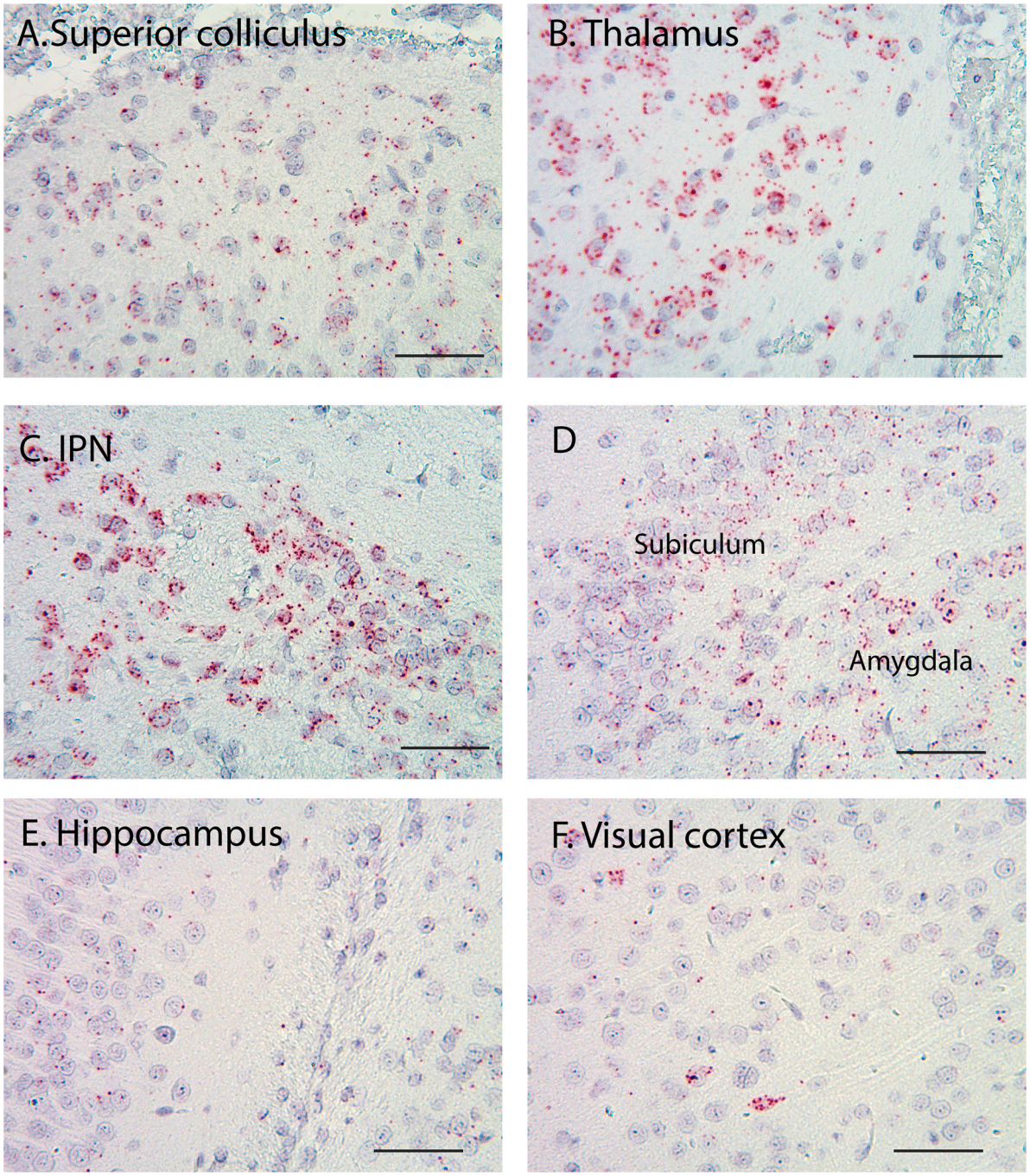

Fig. 10. Higher magnification images of regions enclosed by boxes in Fig. 8. The panels show sensory regions of superior colliculus (A), medial geniculate nucleus of the thalamus (B), interpeduncular nucleus (IPN, C), amygdala and adjacent subiculum (D), CA1 region of hippocampus (E), and layer 5 of anterolateral visual cortex (F). Scale bar = 50 μm.

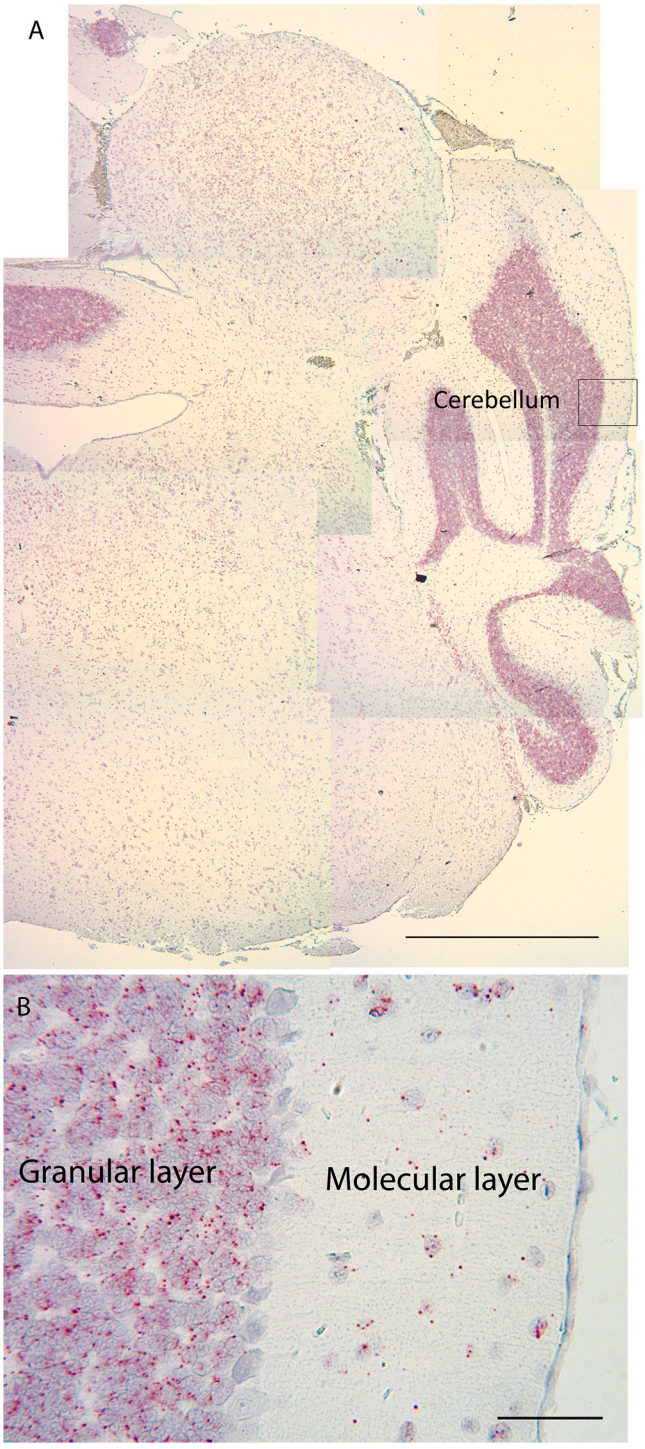

Fig. 11. A) Composite coronal image of cerebellum at level 106 of the Allen Brain Atlas. Scale bar = 0.5 mm. B) Higher magnification image of the region enclosed by the box in A. Cells in the granular and molecular layer were strongly labeled by Syt9 mRNA but adjacent Purkinje cells were not. Scale bar = 50 μm.

important site for regulating relapse in addictive behaviors (Childs et al., 2024). Genetic manipulation of Syt9 expression (Quadros et al., 2017) might therefore offer a promising target for regulating these behaviors.

The choroid plexus within the ventricles showed surprisingly strong Syt9 mRNA expression. Ependymal cells that line ventricles did not show elevated expression. The choroid plexus consists of both capillary endothelial cells and neuroepithelial cells that secrete cerebrospinal fluid into the ventricles. Neuroepithelial cells originate from neuroectoderm during development and thus seem more likely than endothelial cells to express high levels of Syt9 mRNA. Secretion of CSF is driven by the activity of ion transporters, but this activity can be regulated by intracellular Ca^{2+} levels (Macaulay and Toft-Bertelsen (2023)). Syt9 might therefore be involved in regulating CSF secretion, as well as regulating neurotransmitter release in various sensory and limbic regions.

CRediT authorship contribution statement

Boateng Kwadwo O.: Writing – original draft, Investigation. **Thoreson Wallace B:** Writing – original draft, Supervision, Funding acquisition, Formal analysis, Data curation, Conceptualization. **Stauch Kelly L.:** Methodology. **Hadford Lucian D.:** Writing – review & editing, Investigation. **Kincaid Anthony E.:** Writing – review & editing, Formal analysis, Data curation.

Funding

This work was supported by NIH EY10542 (WBT), EY32396 (WBT), NE-INBRE Summer Fellowship to L. Hadford (5P20GM103427), UNMC Graduate Studies (KB).

Declaration of Competing Interest

The authors declare that they have no known competing financial interests or personal relationships that could have appeared to influence the work reported in this paper.

References

Bhalla, A., Chicka, M.C., Tucker, W.C., Chapman, E.R., 2006. Ca(2+)-synaptotagmin directly regulates t-SNARE function during reconstituted membrane fusion. Nat. Struct. Mol. Biol. 13, 323–330.
Bhalla, A., Tucker, W.C., Chapman, E.R., 2005. Synaptotagmin isoforms couple distinct ranges of Ca2+ , Ba2+ , and Sr2+ concentration to SNARE-mediated membrane fusion. Mol. Biol. Cell 16, 4755–4764.
Brose, N., Petrenko, A.G., Sudhof, T.C., Jahn, R., 1992. Synaptotagmin: a calcium sensor on the synaptic vesicle surface. Science 256, 1021–1025.
Carey, M.R., 2024. The cerebellum. Curr. Biol. 34, R7–R11.
Childs, J.E., Morabito, S., Das, S., Santelli, C., Pham, V., Kusche, K., Vera, V.A., Reese, F., Campbell, R.R., Matheos, D.P., Swarup, V., Wood, M.A., 2024. Relapse to cocaine seeking is regulated by medial habenula NR4A2/NURR1 in mice. Cell Rep. 43, 113956.
Craxton, M., 2010. A manual collection of Syt, Esyt, Rph3a, Rph3al, Doc2, and Dblc2 genes from 46 metazoan genomes–an open access resource for neuroscience and evolutionary biology. BMC Genom. 11, 37.
Fernandez-Chacon, R., Konigstorfer, A., Gerber, S.H., Garcia, J., Matos, M.F., Stevens, C. F., Brose, N., Rizo, J., Rosenmund, C., Sudhof, T.C., 2001. Synaptotagmin I functions as a calcium regulator of release probability. Nature 410, 41–49.
Geppert, M., Goda, Y., Hammer, R.E., Li, C., Rosahl, T.W., Stevens, C.F., Sudhof, T.C., 1994. Synaptotagmin I: a major Ca2+ sensor for transmitter release at a central synapse. Cell 79, 717–727.
Hui, E., Bai, J., Wang, P., Sugimori, M., Llinas, R.R., Chapman, E.R., 2005. Three distinct kinetic groupings of the synaptotagmin family: candidate sensors for rapid and delayed exocytosis. Proc. Natl. Acad. Sci. USA 102, 5210–5214.
Lee, H.W., Yang, S.H., Kim, J.Y., Kim, H., 2019. The role of the medial habenula cholinergic system in addiction and emotion-associated behaviors. Front Psychiatry 10, 100.
Li, C., Ullrich, B., Zhang, J.Z., Anderson, R.G., Brose, N., Sudhof, T.C., 1995. Ca(2+)-dependent and -independent activities of neural and non-neural synaptotagmins. Nature 375, 594–599.
Macaulay, N., Toft-Bertelsen, T.L., 2023. Dual function of the choroid plexus: cerebrospinal fluid production and control of brain ion homeostasis. Cell Calcium 116, 102797.
Mackler, J.M., Drummond, J.A., Loewen, C.A., Robinson, I.M., Reist, N.E., 2002. The C (2)B Ca(2+)-binding motif of synaptotagmin is required for synaptic transmission in vivo. Nature 418, 340–344.
Mathis, V., Kenny, P.J., 2019. From controlled to compulsive drug-taking: the role of the habenula in addiction. Neurosci. Biobehav Rev. 106, 102–111.
Mclaughlin, I., Dani, J.A., Biasi, M, D.E., 2017. The medial habenula and interpeduncular nucleus circuitry is critical in addiction, anxiety, and mood regulation. J. Neurochem. 142 (2), 130–143.
Mesnard, C.S., Hays, C.L., Townsend, L.E., Barta, C.L., Gurumurthy, C.B., Thoreson, W.B., 2024. Synaptotagmin-9 in mouse retina. Vis. Neurosci. 41, E003.

Mittelsteadt, T., Seifert, G., Alvarez-Baron, E., Steinhauser, C., Becker, A.J., Schoch, S., 2009. Differential mRNA expression patterns of the synaptotagmin gene family in the rodent brain. J. Comp. Neurol. 512, 514–528.

Moberg, S., Takahashi, N., 2022. Neocortical layer 5 subclasses: from cellular properties to roles in behavior. Front Synaptic Neurosci. 14, 1006773.

Monies, D., Abouelhoda, M., Alsayed, M., Alhassnan, Z., Alotaibi, M., Kayyali, H., AL-Owain, M., Shah, A., Rahbeeni, Z., Al-Muhaizea, M.A., Alzaidan, H.I., Cupler, E., Bohlega, S., Faqeih, E., Faden, M., Alyounes, B., Jaroudi, D., Goljan, E., Elbardisy, H., Akilan, A., Albar, R., Aldhalaan, H., Gulab, S., Chedrawi, A., Al Saud, B.K., Kurdi, W., Makhseed, N., Alqasim, T., El Khashab, H.Y., Al-Mousa, H., Alhashem, A., Kanaan, I., Algoufi, T., Alsaleem, K., Basha, T.A., Al-Murshedi, F., Khan, S., Al-Kindy, A., Alnemer, M., Al-Hajjar, S., Alyamani, S., Aldhekri, H., Al-Mehaidib, A., Arnaout, R., Dabbagh, O., Shagrani, M., Broering, D., Tulbah, M., Alqassmi, A., Almugbel, M., Alquaiz, M., Alsaman, A., Al-Thihli, K., Sulaiman, R.A., Al-Dekhail, W., Alsaegh, A., Bashiri, F.A., Qari, A., Alhomadi, S., Alkuraya, H., Alsebayel, M., Hamad, M.H., Szonyi, L., Abaalkhail, F., Al-Mayouf, S.M., Almojalli, H., Alqadi, K.S., Elsiesy, H., Shuaib, T.M., Seidahmed, M.Z., Abosoudah, I., Akleh, H., Alghonaium, A., Alkharfy, T.M., Al Mutairi, F., Eyaid, W., Alshanbary, A., Sheikh, F.R., Alsohaibani, F.I., Alsonbul, A., Al Tala, S., Balkhy, S., Bassiouni, R., Alenizi, A.S., Hussein, M.H., Hassan, S., Khalil, M., Tabarki, B., Alshahwan, S., Oshi, A., Sabr, Y., Alsaadoun, S., Salih, M.A., Mohamed, S., Sultana, H., Tamim, A., El-Haj, M., Alshahrani, S., Bubshait, D.K., Alfadhel, M., et al., 2017. The landscape of genetic diseases in saudi arabia based on the first 1000 diagnostic panels and exomes. Hum. Genet 136, 921–939.

Nagayama, S., Homma, R., Imamura, F., 2014. Neuronal organization of olfactory bulb circuits. Front Neural Circuits 8, 98.

Pang, Z.P., Melicoff, E., Padgett, D., Liu, Y., Teich, A.F., Dickey, B.F., Lin, W., Adachi, R., Sudhof, T.C., 2006. Synaptotagmin-2 is essential for survival and contributes to Ca2 + triggering of neurotransmitter release in central and neuromuscular synapses. J. Neurosci. 26, 13493–13504.

Pinheiro, P.S., Houy, S., Sorensen, J.B., 2016. C2-domain containing calcium sensors in neuroendocrine secretion. J. Neurochem. 139, 943–958.

Quadros, R.M., Miura, H., Harms, D.W., Akatsuka, H., Sato, T., Aida, T., Redder, R., Richardson, G.P., Inagaki, Y., Sakai, D., Buckley, S.M., Seshacharyulu, P., Batra, S.K., Behlke, M.A., Zeiner, S.A., Jacobi, A.M., Izu, Y., Thoreson, W.B., Urness, L.D., Mansour, S.L., Ohtsuka, M., Gurumurthy, C.B., 2017. Easi-CRISPR: a robust method for one-step generation of mice carrying conditional and insertion alleles using long ssDNA donors and CRISPR ribonucleoproteins. Genome Biol. 18, 92.

Seibert, M.J., Evans, C.S., Stanley, K.S., Wu, Z., Chapman, E.R., 2023. Synaptotagmin 9 modulates spontaneous neurotransmitter release in striatal neurons by regulating substance P secretion. J. Neurosci. 43, 1475–1491.

Sugita, S., Shin, O.H., Han, W., Lao, Y., Sudhof, T.C., 2002. Synaptotagmins form a hierarchy of exocytotic Ca(2+) sensors with distinct Ca(2+) affinities. EMBO J. 21, 270–280.

Verhage, M., Sorensen, J.B., 2020. SNAREopathies: diversity in Mechanisms and Symptoms. Neuron 107, 22–37.

Wolfes, A.C., Dean, C., 2020. The diversity of synaptotagmin isoforms. Curr. Opin. Neurobiol. 63, 198–209.

Xu, J., Mashimo, T., Sudhof, T.C., 2007. Synaptotagmin-1, -2, and -9: Ca(2+) sensors for fast release that specify distinct presynaptic properties in subsets of neurons. Neuron 54, 567–581.